Environmental Technology & Innovation 20 (2020) 101093

Contents lists available at ScienceDirect

Environmental Technology & Innovation

journal homepage: www.elsevier.com/locate/eti

Surface innovation to enhance anti-droplet and hydrophobic behavior of breathable compressed-polyurethane masks

Saikat Sinha Ray [a], You-In Park [b], Hosik Park [b], Seung-Eun Nam [b], In-Chul Kim [b], Young-Nam Kwon [a,*]

[a] School of Urban and Environmental Engineering (UEE), Ulsan National Institute of Science and Technology (UNIST), Republic of Korea

[b] Membrane Research Center, Korea Research Institute of Chemical Technology, Daejeon, Republic of Korea

ARTICLE INFO

Article history:
Received 15 July 2020
Received in revised form 3 August 2020
Accepted 3 August 2020
Available online 7 August 2020

Keywords:
COVID-19
Face mask
Polyurethane
Silica sol
Hexadecyltrimethoxysilane
Anti-droplet

ABSTRACT

With the emergence of the coronavirus disease (COVID-19), it is essential that face masks demonstrating significant anti-droplet and hydrophobic characteristics are developed and distributed. In this study, a commercial compressed-polyurethane (C-PU) mask was modified by applying a hydrophobic and anti-droplet coating using a silica sol, which was formed by the hydrolysis of tetraethoxysilane (TEOS) under alkaline conditions and hydrolyzed hexadecyltrimethoxysilane (HDTMS) to achieve hydrophobization. The modified mask (C-PU/Si/HDTMS) demonstrated good water repellency resulting in high water contact angle (132°) and low sliding angle (17°). Unmodified and modified masks were characterized using attenuated total reflection-Fourier transform infrared (ATR-FTIR) spectroscopy, scanning electron microscopy (SEM), energy-dispersive X-ray spectroscopy (EDS), and X-ray photoelectron spectroscopy (XPS). A drainage test confirmed the strong interaction between the mask surface and coating. Moreover, the coating had negligible effect on the average pore size of the C-PU mask, which retained its high breathability after modification. The application of this coating is a facile approach to impart anti-droplet, hydrophobic, and self-cleaning characteristics to C-PU masks.

1. Introduction

As per 4 recent reports from the World Health Organization (WHO), viral diseases present a serious problem to public health. In the last two decades, several virus-related epidemic diseases, such as the severe acute respiratory syndrome coronavirus (SARS-CoV) during the early 2000s (2002–03), as well as the H1N1 influenza in 2009, were recorded. More recently, an unexplained respiratory disease was first reported to the WHO country office in China during late December 2019. According to reports, the etiology of this disease was attributed to a novel virus belonging to the coronavirus family (CoV). Two months later (February 2020), the WHO Director-General, Dr. Tedros Adhanom Ghebreyesus, announced that the disease caused by this new coronavirus family was named "COVID-19", which is an acronym for coronavirus disease 2019 (Cascella et al., 2020; Sohrabi et al., 2020; Nishiura et al., 2020).

COVID-19 is highly infectious, with symptoms including respiratory distress, weakness, dry cough, and high fever; however, most of those infected remain asymptomatic. Existing reports indicate that virus transmission typically occurs

* Corresponding author.
E-mail address: kwonyn@unist.ac.kr (Y.-N. Kwon).

https://doi.org/10.1016/j.eti.2020.101093
2352-1864/

via respiratory droplets produced by sneezing and coughing (W.H. Organization, 2020; Rothan and Byrareddy, 2020). Facial masks offer a physical barrier against water spatter or respiratory droplets. In addition, facial masks reduce hand-to-mouth or hand-to-nose transmission. One of the greatest challenges in public health has been preventing people from touching their faces, as the nose, eyes, and mouth are all potential entry points for SARS-CoV-2, the virus that causes COVID-19, and many other germs (MacIntyre et al., 2009; Eikenberry et al., 2020).

The shortage of effective, anti-droplet face masks during the COVID-19 pandemic has become a significant issue for every country due to the sudden increase in demand. In Taiwan, government regulations stipulated that a person may have only 2 masks per week during early March 2020 (El-Atab et al., 2020). Several types of commercially available face masks offer different degrees of protection, but most are hydrophilic and ineffective when wet. Research indicates that if a mask gets wet, its effectiveness in blocking water spatter or accommodating proper respiration decreases (Anon, 2020; Nazeeri et al., 2020).

In order to address these issues, a modified compressed-polyurethane (C-PU) face mask has been produced with anti-droplet and hydrophobic properties for long-term usage. Commercial polyurethane masks have been popular during this pandemic owing to attractive properties such as flexibility, comfort, softness, and excellent blockage to particulates. Typically, compressed polyurethane mask consists of 3-D mesh structure that blocks 99% of pollen sized particles. This mask is based on porous filter technology which controls the pores to form the ideal density and size for trapping pollen sized particles. In addition to that, it can be reused even after 2–3 washes. Above all, it is highly cheap and commercially available that delivers overwhelming air permeability. Nonetheless, due to high water absorbency as a result of the hydrophilicity of the masks diminishes their water-repelling properties but may be solved by a coating that imparts hydrophobic as well as anti-droplet features. In this study, a simple fabrication approach was demonstrated wherein tetraethyl orthosilicate (TEOS) is hydrolyzed in a H_2O/ethanol solution mixture to form silane sol and hexadecyltrimethoxysilane (HDTMS) is hydrolyzed in ethanol solution to form an alkylsilanol. Until now, fluorinated based material or coating has been used as one of the effective agents for lowering the surface free energy. But recent research suggests that, fluorinated materials are expensive as well as not environmentally friendly (Xu et al., 2015). In this study, a non-fluoro compound, hexadecyltrimethoxysilane (HDTMS), an organosilane with a C-16 hydrocarbon tail, has been utilized to modify the surface of silica. Typically, HDTMS is an amphiphilic molecule consisting of hydrophilic head where a central silicon atom is attached to three -OCH_3 groups, and its hydrophobic tail is composed of an alkyl chain formed by a straight succession of fifteen CH_2 groups and one CH_3 group at its end. The results in long-chain alkylsilane with low surface free energy has been introduced onto SiO_2 grafted surfaces, hence, generating the modified hydrophobic surface (Xu et al., 2012).

The C-PU mask sample was first treated with the silica sol and then the same sample was immersed in the hydrolyzed HDTMS solution before drying and curing. The self-assembly of the HDTMS is a result of the counteraction among the alkylsilanol and the surface hydroxyl groups of silica nanoparticles onto the C-PU surface (Ammayappan et al., 2020). Now as far as the practical feasibility is concerned, a hydrophobic anti-droplet mask surface has been fabricated by utilizing dip coating process. Typically, dip coating is a low cost, facile and most reliable technique that involves the deposition of liquid by immersing the (mask) substrate into the solution (silica sol and HDTMS solution) consisting of metal compounds that undergo hydrolysis. After taking out the substrate (mask) from the above solution(s), a homogeneous liquid film is formed on the substrate's surface. Recent studies suggest that, dip coating is an industrial coating technique which is considered to be one of the highly reproducible methods (Neacşu et al., 2016). Scheme 1 illustrates the mechanism involved in the silica sol modification of a face mask (C-PU), followed by a hydrophobization treatment using HDTMS.

Different categories of masks have shown success in minimizing the virus transmission associated with water spatter or droplets. However, there are limited mask materials that offer protection against water because waterproof mask materials are seldom breathable (Baji et al., 2020). Moreover, there are certain disadvantages to wearing hydrophilic masks, such as self-contamination with wet hands. Contamination can occur if the mask becomes wet, which can promote the growth of microorganisms and lead to discomfort due to low breathability.

As far as the structural aspect is concerned, the inner spongy layer is kept unchanged and was found to be hydrophilic in nature that helps in absorbing moisture. In addition to that, the compressed polyurethane masks are non-allergic in nature that are comfortable with face/skin. However, the outer layer has been chemically modified that was observed to be hydrophobic for droplet/ splash resistance application. Moreover, the porous structure demonstrates the capability of high air permeability. Thus, this dual layer concept has been applied in the present study to reduce the chance of contamination from water droplets or splashes. Fig. 1 illustrates the structural aspect of the modified mask (C-PU/Si/HDTMS) for anti-droplet application.

In this study, a hydrophobic mask coating was developed with wetting resistance and self-cleaning features. A simple protocol is presented wherein a flexible, stable, reusable, and economical C-PU mask is subjected to environmental engineering processes (Allison et al., 2020; Xie et al., 2020). This study conducted fundamental research into the development of hydrophobic and anti-droplet masks. The hydrophobicity and wettability of mask surface has been thoroughly evaluated. In general, wettability is not analyzed by contact angle (θ) only. There is another crucial element i.e. contact angle hysteresis (CAH) that characterizes wetting state of the surface. The contact angle hysteresis indicates how water droplets behave. In the case of a water droplet, the sliding only begins when the shape of droplet becomes asymmetric, and only when enough high force is exerted. Thus, contact angle, contact angle hysteresis (CAH), as well as sliding angle are the important factors of analyzing wetting state (Makkonen, 2017). Unmodified and modified masks were

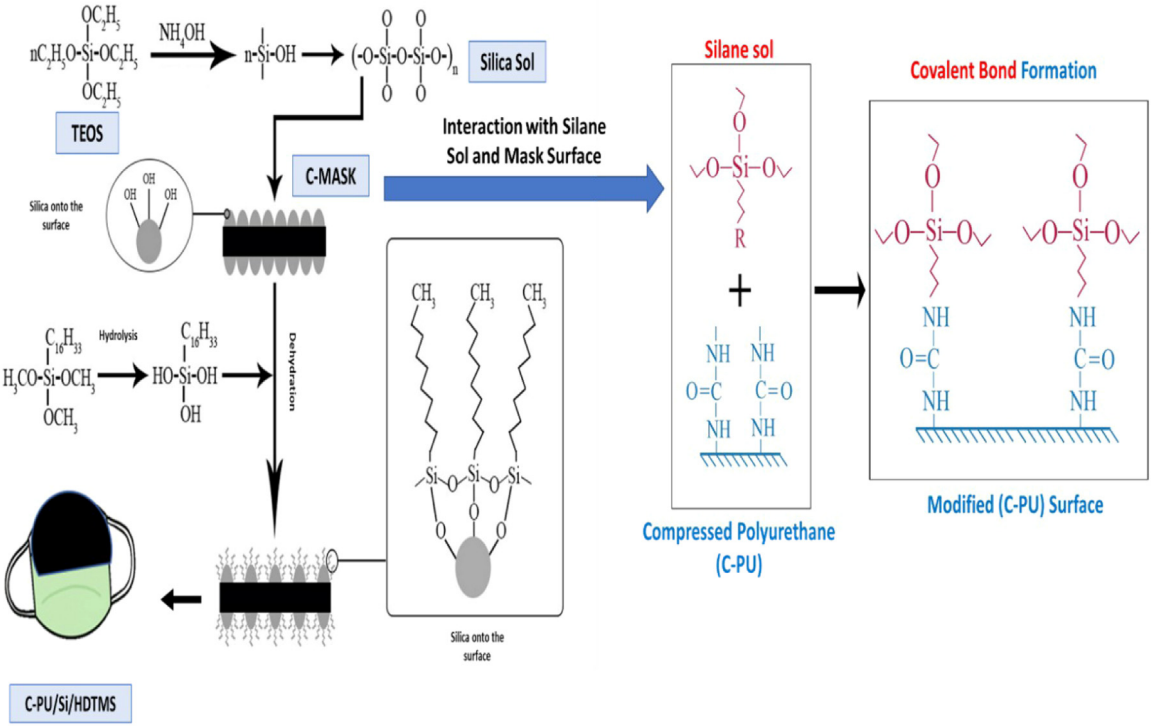

Scheme 1. Reaction of silica sol with compressed polyurethane (C-PU) mask followed by hydrophobization treatment using HDTMS.

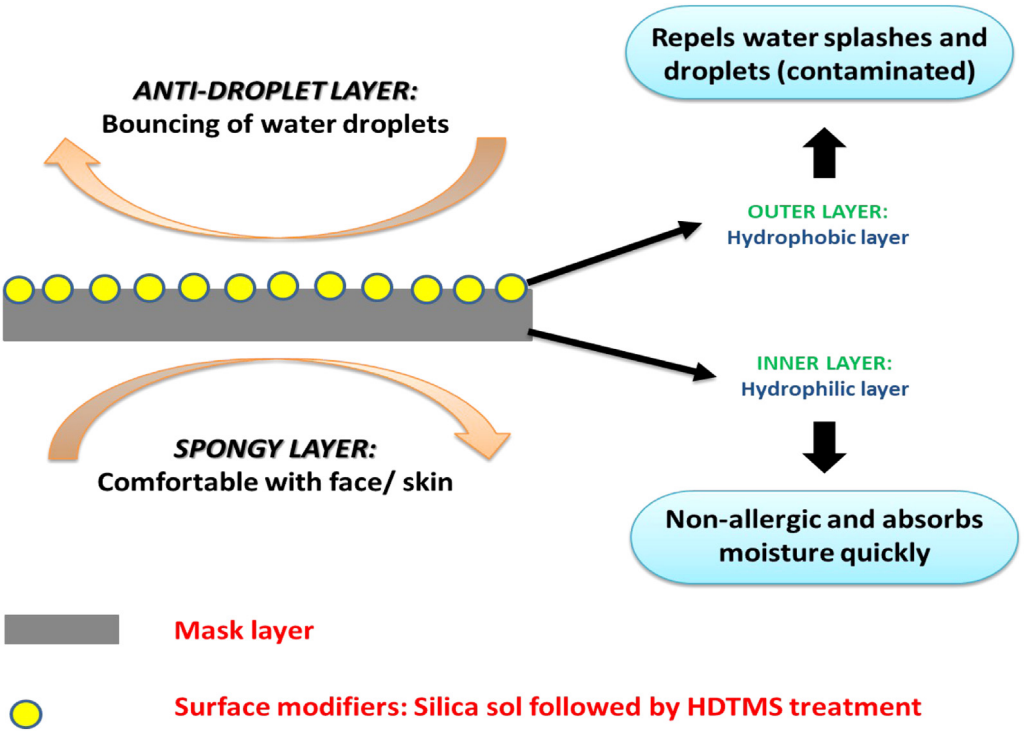

Fig. 1. Structural aspect of the modified mask for splash resistant application.

characterized using an optical contact angle measuring device, attenuated total reflection-Fourier transform Infrared (ATR-FTIR) spectroscopy, scanning electron microscopy (SEM), energy-dispersive X-ray spectroscopy (EDS), X-ray photoelectron spectroscopy (XPS) and inductively coupled plasma mass spectrometry (ICP-MS). Unmodified and modified masks were subjected to drainage tests, and their wetting and self-cleaning properties were evaluated using sliding angle tests.

2. Materials and methods

2.1. Materials

Compressed-polyurethane (C-PU) comfort masks were acquired from Korea. Reagent-grade ammonium hydroxide (NH_4OH) (Alfa Aesar), tetraethyl orthosilicate (TEOS) (Sigma), hexadecyltrimethoxysilane (HDTMS) (Sigma-Aldrich), and ethyl alcohol (Solvay) were acquired and utilized without further purification.

2.2. Preparation of silica sol

The silica sol has been prepared through alkaline hydrolysis of TEOS in an ammonium hydroxide and ethyl alcohol solution. The NH_4OH (3 and 6 mL, respectively) was gradually added to the ethanol solvent (100 mL) while continuously stirring at 60 °C for half an hour. Subsequently, 6 ml of TEOS has been added dropwise to the former solution, and the solution was constantly stirred for one and half hour to produce the silica sol.

2.3. HDTMS Solution preparation

HDTMS (4%, v/v) was gradually added to an ethanol solvent and then continuously stirred for one hour in order to generate an alkylsilanol solution.

2.4. Mask coating

After successful preparation of the silica sol and HDTMS solution, a mask (C-PU) sample has been sonicated in a silica sol placed in a bath sonicator for half an hour to ensure uniform coating of silica sol, then partially dried at room temperature followed by drying at 75 °C for 5 min. After drying, the silica sol treated specimens have been sonicated in the HDTMS solution for one hour. Typically, sonication by bath sonicator can generate uniform sized small droplets in batch and production process, that provides excellent control over the final particle size. The samples were dried at 25 °C for 12 h and then cured at 100 °C for 3 min. Refer to Fig. 2 for a schematic representation of the anti-droplet mask fabrication process.

2.5. Material characterization

The number-percent based on nanoparticle sizes of the silica sol sample were analyzed by using a particle size analyzer (Zetasizer Nano ZS, UK) 60 min after sol samples (Si-1 and Si-2) were prepared. The transformed morphology of the masks, resulting from the surface and chemical modifications, was examined using scanning electron microscopy (SEM; Quanta 200 FEG, Netherland (s). Chemical bond modifications and the organic functional chemical groups on the mask surfaces were confirmed using Fourier transform infrared (FTIR) spectroscopy. X-ray photoelectron spectroscopy (XPS; K-Alpha, Thermo Fisher Scientific, USA) has been utilized for chemical characterization of the mask surfaces in order to evaluate the surface modifications. FTIR analysis was conducted using a spectrophotometer (Nicolet 6700, Thermo Scientific) over a resolution range of 650–4000 cm^{-1}. The hydrophobicity and surface wettability of the prepared specimens were measured using a Phoenix 300 Plus instrument (Surface Electro Optics Co., Ltd., Korea). The mean of 3 measurements of deionized (DI) water droplets, at different locations on each sample and using the sessile drop method, was considered to evaluate the average contact angle. In addition, a digital thickness gauge (Mitutoyo, Japan) was used to analyze the thickness of the masks.

2.6. Contact angle hysteresis

The hydrophobicity of the mask surface was evaluated by the sessile drop technique. The advancing contact angle have been measured for small droplet (1 μL/sec) at total frame numbers of 15 with 1 s interval. The maximum advancing contact angle was recorded. After that the water droplet was sucked slowly off 15 μL at a rate of 1 μL/sec and the minimum receding angle was recorded for all mask surfaces. Finally, the contact angle hysteresis (CAH) was also analyzed by utilizing this equation (Guo et al., 2018):

$$\mathrm{CAH} = \theta_A - \theta_R \tag{1}$$

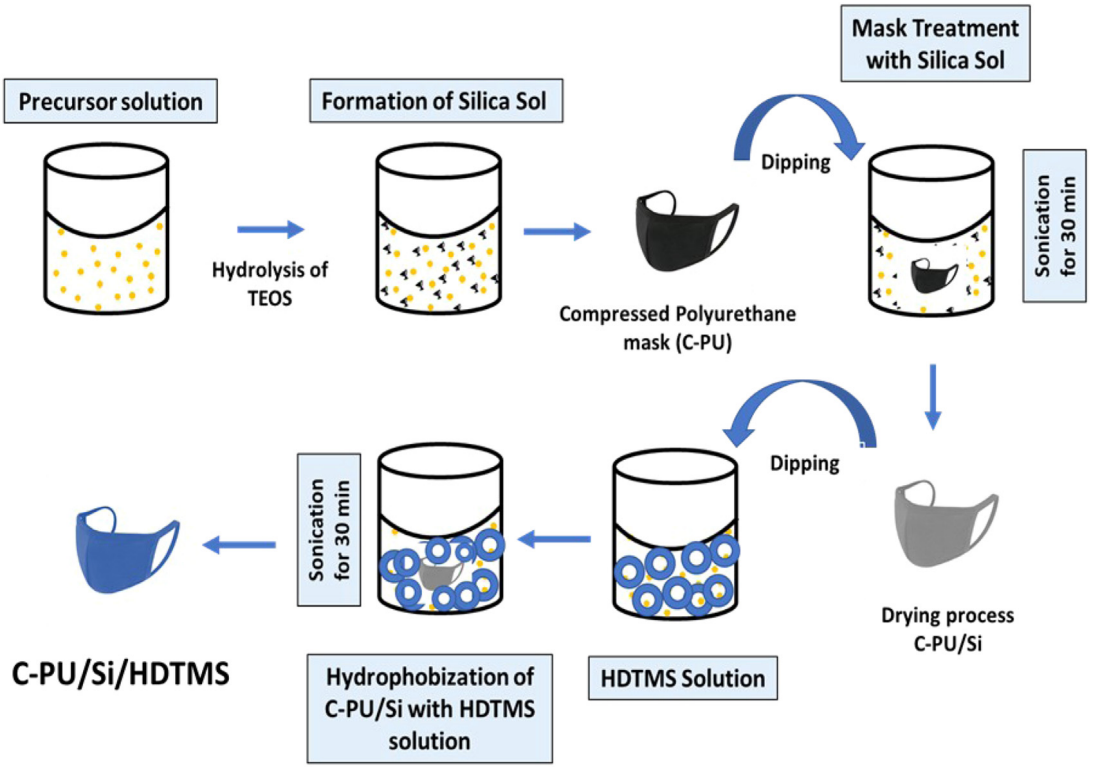

Fig. 2. Graphical representation of mask treatment process to produce a self-cleaning, anti-droplet mask.

Table 1
Formation of silica sol with various concentrations of NH_4OH.

Specimen type	Quantity of TEOS (ml)	Quantity of Ethanol (ml)	Quantity of Ammonium hydroxide (ml)	Polydispersity index (PDI)
Si-1	6 ml	100 ml	3 ml	0.7
Si-2	6 ml	100 ml	6 ml	0.5

2.7. Stability test

The amount of silicon that can be drained from coated masks needs to be analyzed for every type of Si-coated mask in order to evaluate the coating stability. The mask specimens (5 cm × 5 cm) were soaked in DI water for 30 min before expressing the DI water. These solutions were subjected to FTIR analysis and inductively coupled plasma mass spectrometry (ICP-MS) to determine the amount of silicon, and other chemicals, leached.

3. Results and discussions

3.1. Particle size and size distribution of silica sol

The methodology for fabricating a stable hydrophobic coating on a mask surface utilizing silica sol as well as HDTMS is discussed in materials and methods section and summarized in Scheme 1. Silica sol specimens (Si-1 and Si-2) with different particle sizes were synthesized by adjusting the content of NH_4OH while generation of the silica sol as indicated in Table 1. The polydispersity index (PDI) value can be used to evaluate the average uniformity of a particle or nanoparticle dispersion (Clayton et al., 2016; Shajari et al., 2020). Interestingly, values greater than 0.8 indicate low stability for a drug delivery/nano-delivery/colloidal system.

The particle size distribution of the silica samples (Si-1 and Si-2) is shown in Fig. 3. It is evident that the average particle size of the silica sol escalates as the content of NH_4OH is raised, since raising the ammonium hydroxide content advances the aggregation as well as condensation of the silica sol particles. In other words, this can be attributed to the fact that the addition of monomer accelerates the nucleation growth of the particles and results in the aggregation of the particles to form larger particles (Green et al., 2003).

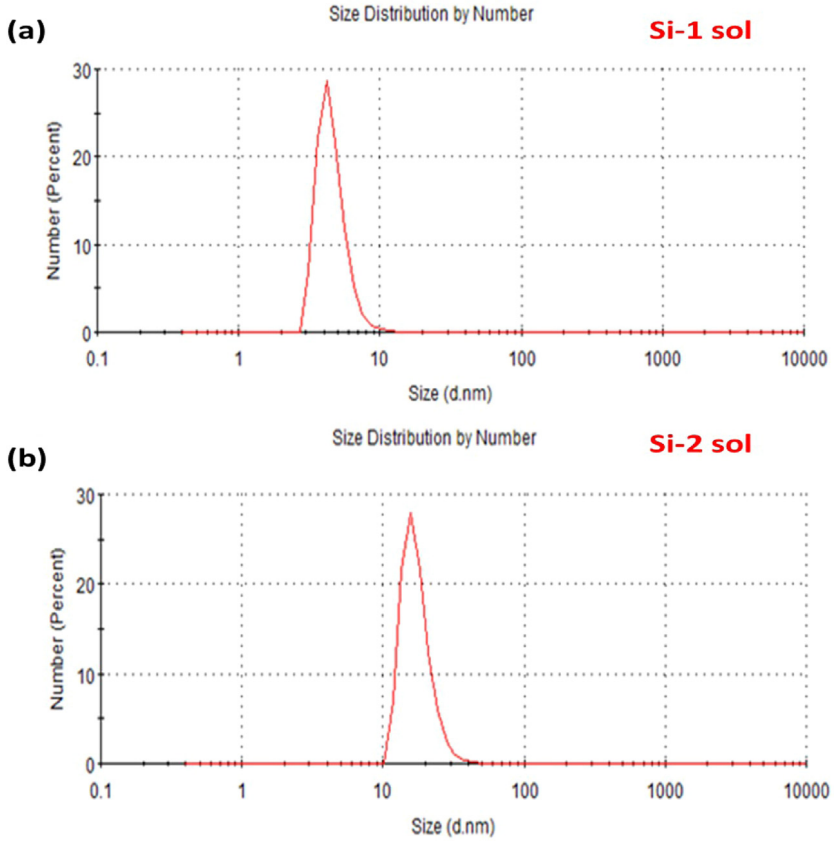

Fig. 3. Number (in percent) of silica nanoparticles (Si-1 and Si-2) as a function of particle size.

3.2. Confirmation of chemical modifications

FTIR spectra of the unmodified C-PU mask and the modified mask (C-PU/Si-1/HDTMS) confirm the polyurethane structure with the typical carbonyl absorption band located at 1725 cm^{-1}, as shown in Fig. 4 (Dias et al., 2010). The absorbance observed at approximately 3335 cm^{-1} is consistent with the stretching of the NH bond, characteristic of urethane and urea groups. In addition, a characteristic band located at 2900 cm^{-1} corresponds to the alkane (-CH) stretching vibration. A strong peak is observed at 1174 cm^{-1} due to the coupling of C–O and C–N stretching vibrations. After modification with silica sol and hydrolyzed with HDTMS, there is an overlapping adsorption band in the C-PU/Si/HDTMS mask peak profile in the wavenumber region of 1052 cm^{-1} that is due to the stretching vibration of Si-O-Si. The Si-O-Si stretching vibration of the modified polyurethane mask was located at 1052 cm-1, although overlapping with the abovementioned absorption band of pristine polyurethane mask surface can be noticed in the FT-IR spectrum (Dias et al., 2010). Furthermore, the Si-C peak is located at approximately 700–755 cm^{-1} (Choi, 2010).

Fig. 5 shows the typical XPS spectra for the C-PU/Si/HDTMS mask. The characteristic peaks at the binding energies of 102.30, 284.22, 400.94, and 531.92 eV correspond to Si 2p, C 1s, N 1s, and O 1s, respectively. It is believed that the nitrogen is shielded with silica (as a result of the modification), which accounts for its low signal intensity.

3.3. Wettability of modified masks

According to Wenzel's model, a low surface energy and high surface roughness are crucial to achieving the maximum contact angle (Sinha Ray et al., 2020; Shakak et al., 2020). In this study, the HDTMS content in the coating resulted in a reduction of the surface energy, promoting hydrophobicity (Wang et al., 2017). As per the Fig. 6, the average water contact angles of modified mask specimens (C-PU/Si/HDTMS) are much higher than that of the unmodified mask (C-PU). In the modified masks, the treatment with the Si/HDTMS solutions contributed to lower surface energies and promoted hydrophobicity. Interestingly, the unmodified mask (C-PU) show a water contact angle of 85° at $t = 0$ min but it reduces to 0° by the time t=15 min, which indicates the highly hydrophilic nature of the unmodified commercial mask. However, the modified masks experience negligible change in water contact angle, even after 15 min. It is worth noting that the C-PU/Si-2/HDTMS mask records a higher water contact angle than the C-PU/Si-1/HDTMS mask, which is ascribed to the

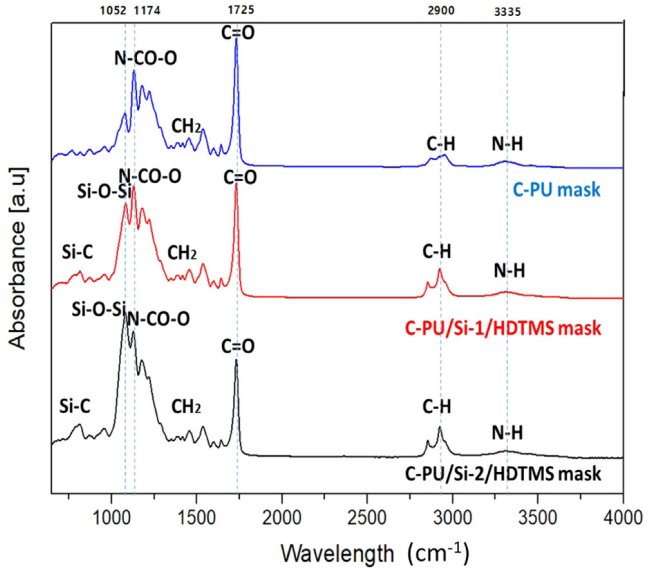

Fig. 4. ATR-FTIR spectra for unmodified and modified masks.

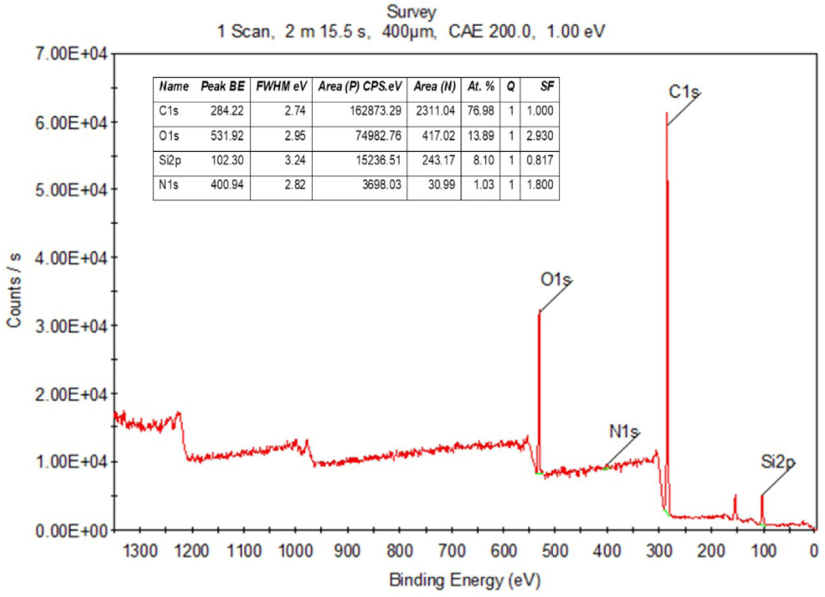

Fig. 5. XPS spectra confirming elemental composition of C-PU/Si/HDTMS mask.

increased aggregation and average particle size of the Si-2 sol (Fig. 3). The C-PU/Si-2/HDTMS mask records a water contact angle of 132° at $t = 0$ min which demonstrates insignificant change, even after 15 min, illustrating the stable hydrophobic nature of the modified mask. It is, therefore, concluded that the treatment of C-PU masks with silica sol and hydrolyzed HDTMS enhances their hydrophobicity.

In general, degree of wetting state and hydrophobicity depends upon varying height from top to base produced from the liquid and the surface. As per Table 2, droplet volume was kept consistent and droplet height has been investigated to examine the degree of wetting state of pristine and modified mask. Interestingly, higher droplet height indicates higher contact angle while keeping the droplet water volume (10 µL) same. This outcome has been found to be consistent as indicated in Fig. 6. Table 2 demonstrates the height from top to base (mm) for pristine and modified mask.

Typically, a sliding angle less than 20° in conjunction with an average water contact angle exceeding 90° indicates hydrophobicity (Tucker et al., 2020). The sliding angle is more important in characterizing the self-cleaning behavior and hydrophobic nature of materials than the maximum achievable average water contact angle (Huang et al., 2013). The

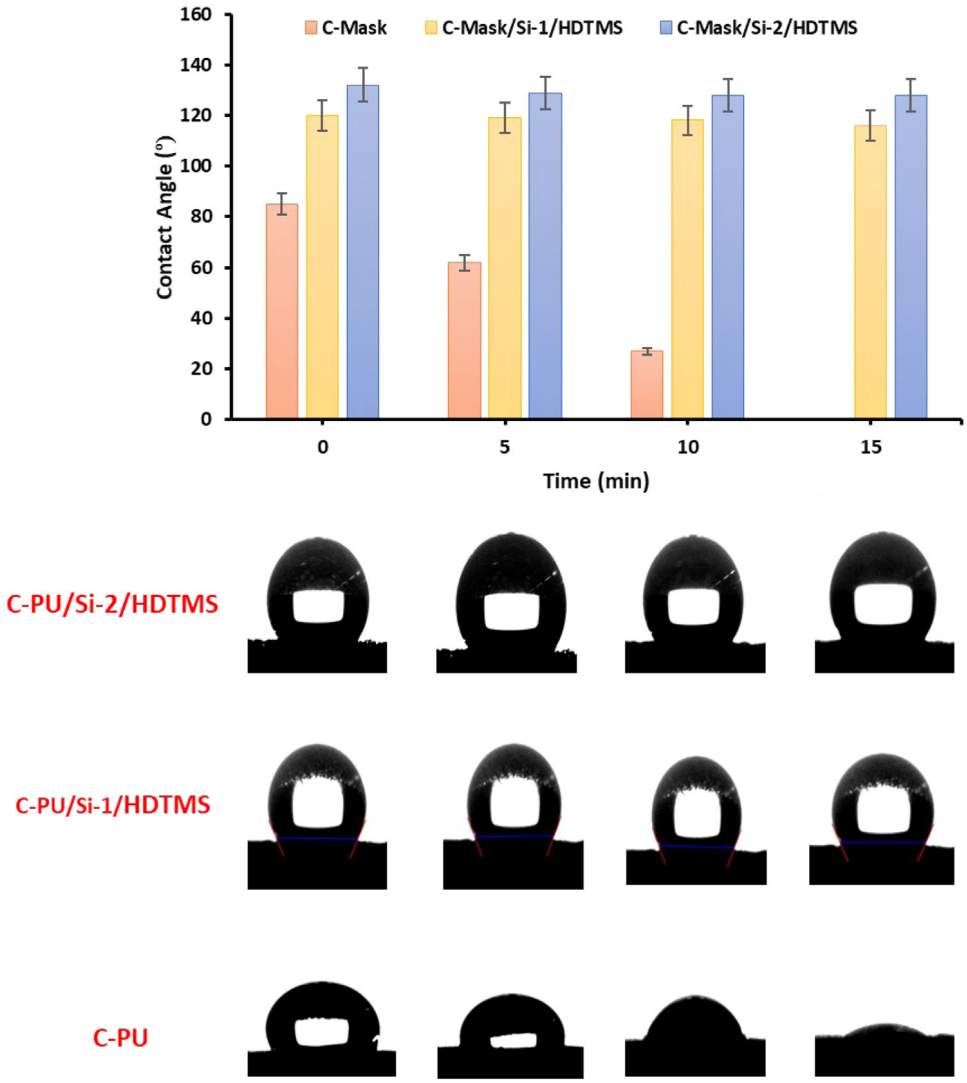

Fig. 6. Evolution of average water contact angles with time. [Note: Droplet volume- 10 μL, Liquid type- DI water and Temperature- 25 °C].

Table 2
Analysis of droplet height for pristine and modified mask.

Mask type	Droplet height (mm)
C-PU	3.54 mm
C-PU/Si-1/HDTMS	4.05 mm
C-PU/Si-2/HDTMS	4.15 mm

sliding angles of the unmodified and modified masks are presented in Fig. 7. The average water contact angle (132°) and the sliding angle (17°) confirms the hydrophobicity of the modified mask (C-PU/Si-2/HDTMS). The relatively low sliding angle (SA) allows water droplets to slide across the mask surface with minimal resistance as a result of the low surface energy of the C-PU/Si/HDTMS. In addition, self-cleaning behavior is induced by the low surface energy coating which repels any sort of foulant or dirt.

3.4. Morphological study of masks

The morphology of unmodified and modified masks was investigated using SEM, refer to Fig. 8. The open pore width was evaluated using imaging tools. The SEM micrographs show that the unmodified mask (C-PU) consists of a combination of smaller and larger cell sizes. Interconnected pores and a porous structure characterize both the unmodified

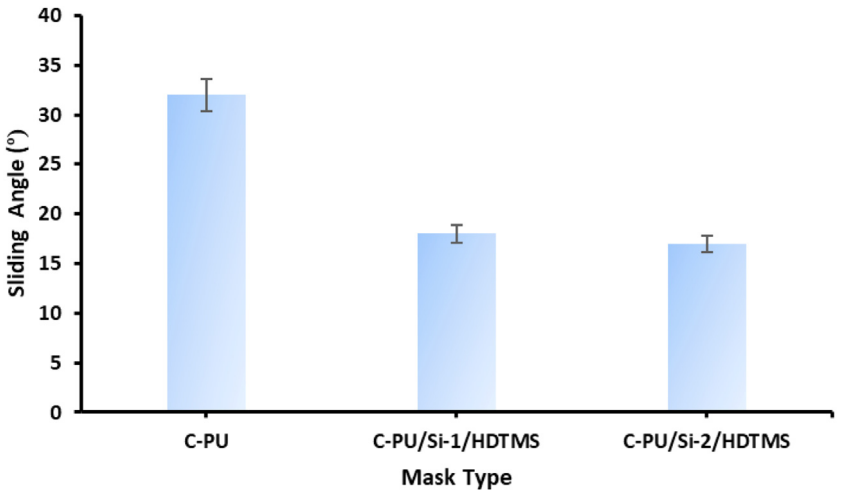

Fig. 7. Sliding angle for various mask surfaces [Note: Droplet volume- 0.5 mL, Liquid type- DI water and Temperature- 25 °C].

Table 3
Thicknesses of unmodified and modified masks.

Mask type	Thickness (μm)
C-PU	470 μm (± 4)
C-PU/Si-1/HDTMS	468 μm (±6)
C-PU/Si-2/HDTMS	469 μm (±5)

and modified masks (Bahrambeygi et al., 2013). Interestingly, the modified mask (C-PU/Si/HDTMS) also shows a porous structure with interconnected pores indicative of highly breathable materials (Baji et al., 2020). A significant portion consists of interconnected open and closed pores, and the walls of the cell are found to be between 25 and 50 μm thick. The open pore width seems to range between 50 to 150 μm for all masks. There is an insignificant change in the morphology of the masks even after surface modification. However, the morphological structure of modified mask becomes less uniform and number of mutilated pores are seen in modified version of C-PU surface. It is, therefore, concluded that the air permeability or breathability of these masks are not significantly changed.

According to the SEM cross sectional view (Fig. 9), the microspheres show oval and spherical morphologies with high porous structure. This porous structure all over the surface indicates higher air permeability that leads to high breathability. In order to examine the internal structure, the cross-sectional morphology has been thoroughly studied that indicates same internal structure for both masks. Typically, high breathable masks demonstrate high air permeability with lower efficiency of droplet blocking (Aydin et al., 2020). However, this facile approach can be utilized as fundamental research where higher permeability can be achieved along with high droplet blocking efficiency.

In addition, SEM-EDX mapping was performed to confirm the carbon, oxygen, and silicon content of the modified mask (C-PU/Si/HDTMS). In Fig. 10, peaks corresponding to carbon and oxygen confirms their presence in the unmodified mask (C-PU). Furthermore, strong peaks for carbon, oxygen, and silicon, are attributed to the silane sol and HDTMS present in the modified masks (C-PU/Si/HDTMS). The EDX mapping indicates that the unmodified mask contains 68.56% carbon and 31.02% oxygen, whereas the modified masks are composed of carbon, oxygen, and silicon, which confirms the successful modification of the compressed polyurethane (C-PU). Interestingly, uniform distributions of carbon, oxygen, and silicon are seen throughout the mask surface, as shown in Fig. 11.

The thickness of the masks was evaluated using a digital thickness gauge at ten different locations and averaged for further calculations. Typically, face masks are made in various thicknesses to protect and act as a barrier against droplets, which affect the breathability and barrier efficacy of the masks. Face masks are considered highly effective in mitigating the spread of diseases and germs via oral or nasal droplets. The thickness of the masks range between 465 and 475 μm (Table 3). There is an insignificant difference between the thickness of the unmodified and modified masks. Thickness plays an important role in how well a filter traps the particles. In most of the mask filters, trapping particles are generally based on "mechanical" collection mechanism that involves inertial impaction, interception and diffusion. This mechanism helps in trapping particles without increasing breathing resistance (Gaurav et al., 2020). Hence, thicker the filter, the better the protection from foreign particles. However, it should not be too thick as it may resist air permeability if the filter is too dense. But, in this study, polyurethane material was found to be extremely porous.

Typically, air permeability or air passage can be defined as the air flow via a given area of a material. This crucial factor is influenced by the porosity of the material, that in turn impacts its openness. The porosity of the material depends

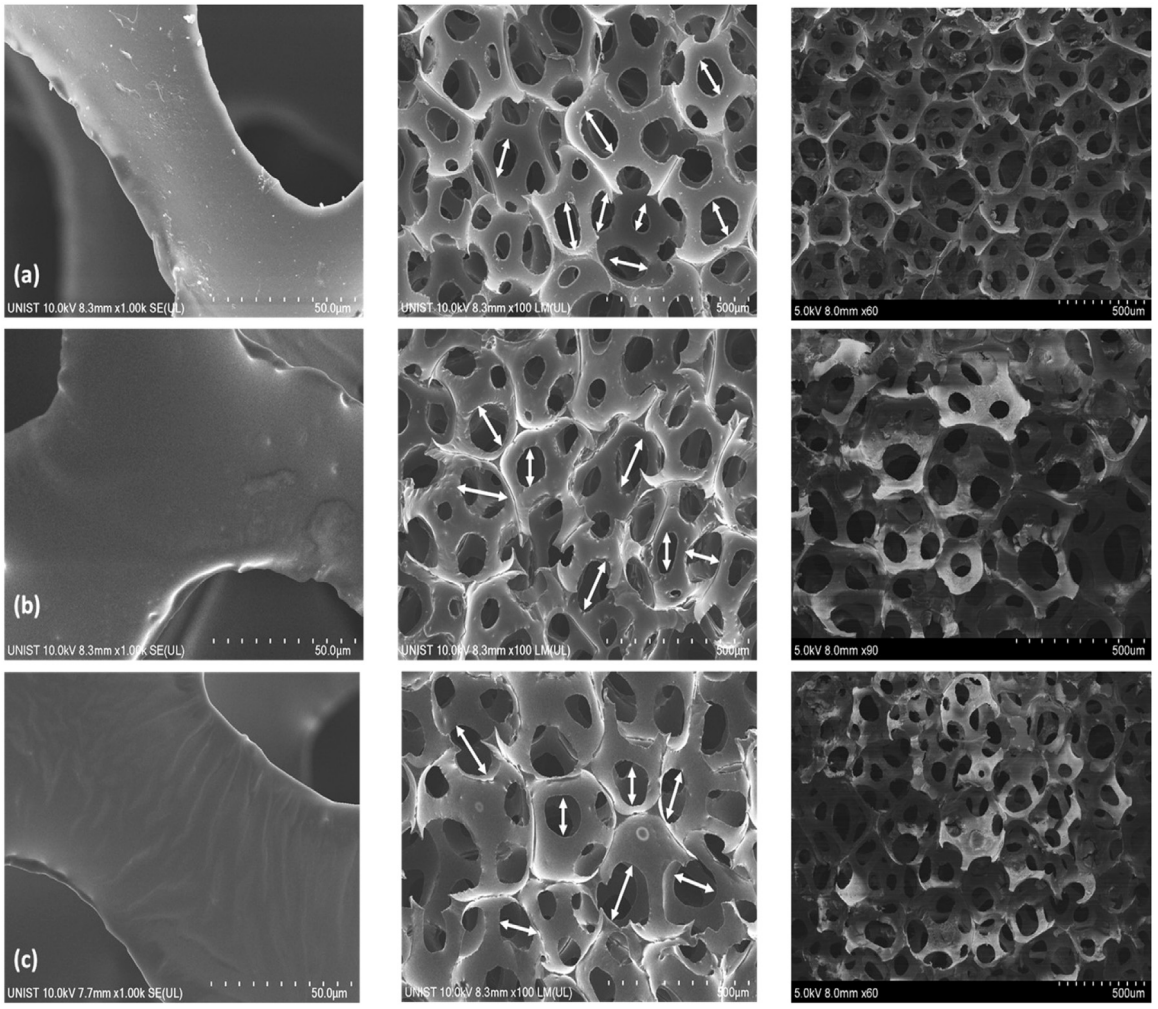

Fig. 8. SEM micrographs of (a) C-PU, (b) C-PU/Si-1/HDMTS, and (c) C-PU/Si-2/HDTMS masks.

upon fabric thickness and density (Mishra and Militky, 2018). Therefore, air permeability can also be correlated based on porosity value.

Material permeability is often evaluated with respect to the porosity of the fabric. The porosity of the material (ε) has been evaluated as follows (Berkalp, 2006):

$$\varepsilon = \frac{(\mathrm{Wwet} - \mathrm{Wdry}) \times 100}{\rho\mathrm{water} \times \mathrm{A} \times \mathrm{h}} \tag{2}$$

where W_{wet} and W_{dry} represent the weights of the wet and dried material (g); ρ_{water} represents water density in g/cm^3; whereas; A and h indicate the area (cm^2) and thickness (cm), respectively, of the material. Fig. 12 shows the measured porosity of various mask materials. Interestingly, the commercial compressed mask indicates very high porosity value of 89.2% compared to that of modified masks (73%–75%). The high porous structure in terms of porosity value indicates high air permeability efficiency. The slight decrease in porosity of modified membrane can be attributed to the modification of silica nanoparticles and surface modifiers which would have reduced or mutilated the pore structure.

3.5. Analysis of contact angle hysteresis (CAH)

Typically, facets of real surfaces such as surface roughness and chemical heterogeneity, may give rise to contact angle hysteresis between an advancing contact angle and a receding contact angle. Therefore, experimental parameters including the equilibrium contact angle Θ e, or the advancing θ_A and receding θ_R contact angles, are considered to analyze the state of wettability of real surfaces. In general, the advancing contact angle indicates the maximum contact angle of the solid surface whereas, the receding illustrates the minimum contact angle of the surface. In addition to that, contact

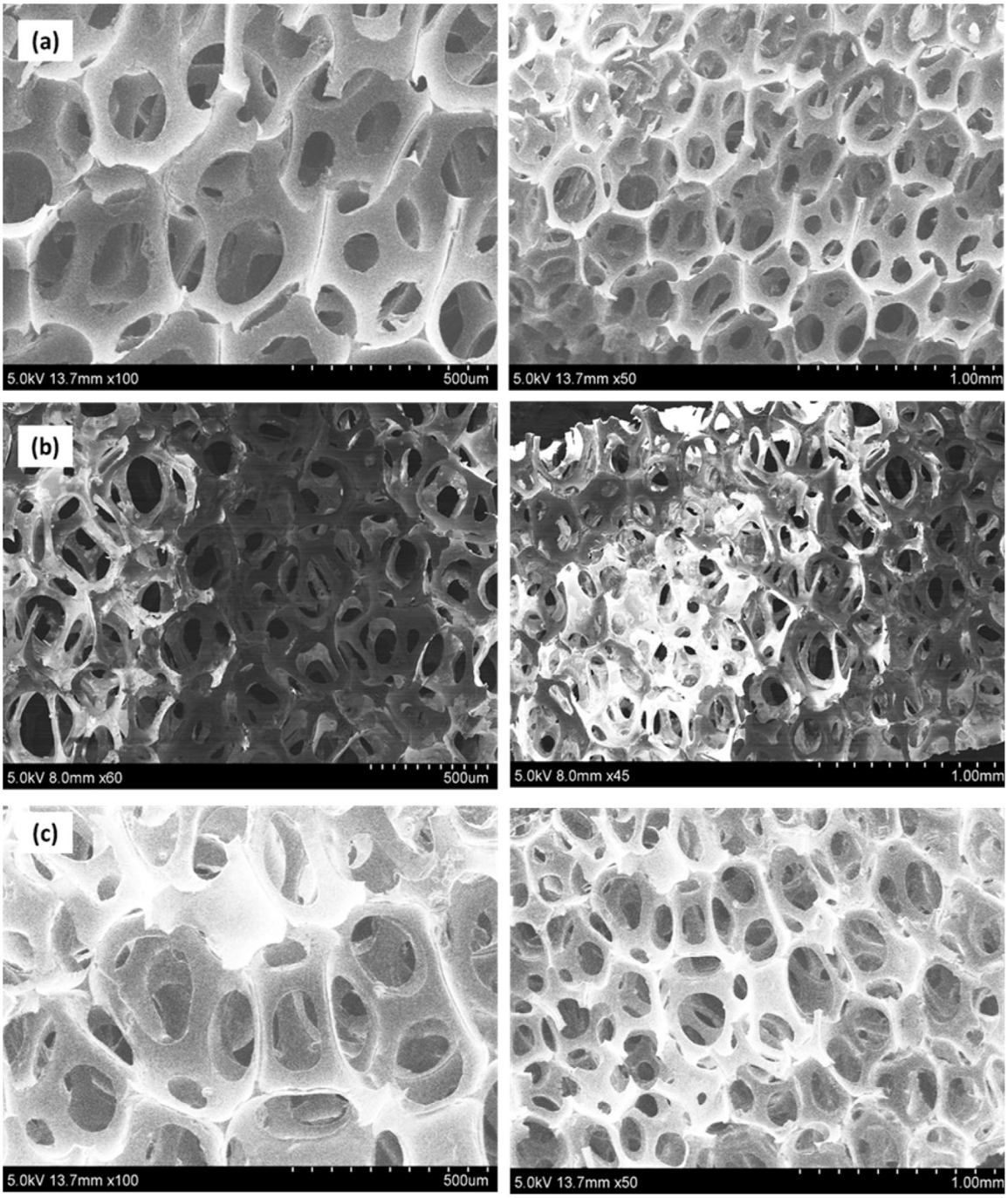

Fig. 9. Cross sectional view of (a) pristine mask (C-PU); (b) modified mask (C-PU/Si-1/HDTMS) and (c) modified mask (C-PU/Si-2/HDTMS) in high and low magnification.

angle hysteresis also demonstrates the degree of drop adhesion onto a solid surface, since in most of the cases, it was found that the higher contact angle hysteresis possesses stronger drop adhesion (Marmur et al., 2017). The contact angle hysteresis has been analyzed for all the mask surfaces and indicated in Fig. 13. Interestingly, low contact angle hysteresis was observed for the modified mask surface compared to that of pristine mask surface that shows lower droplet adhesion.

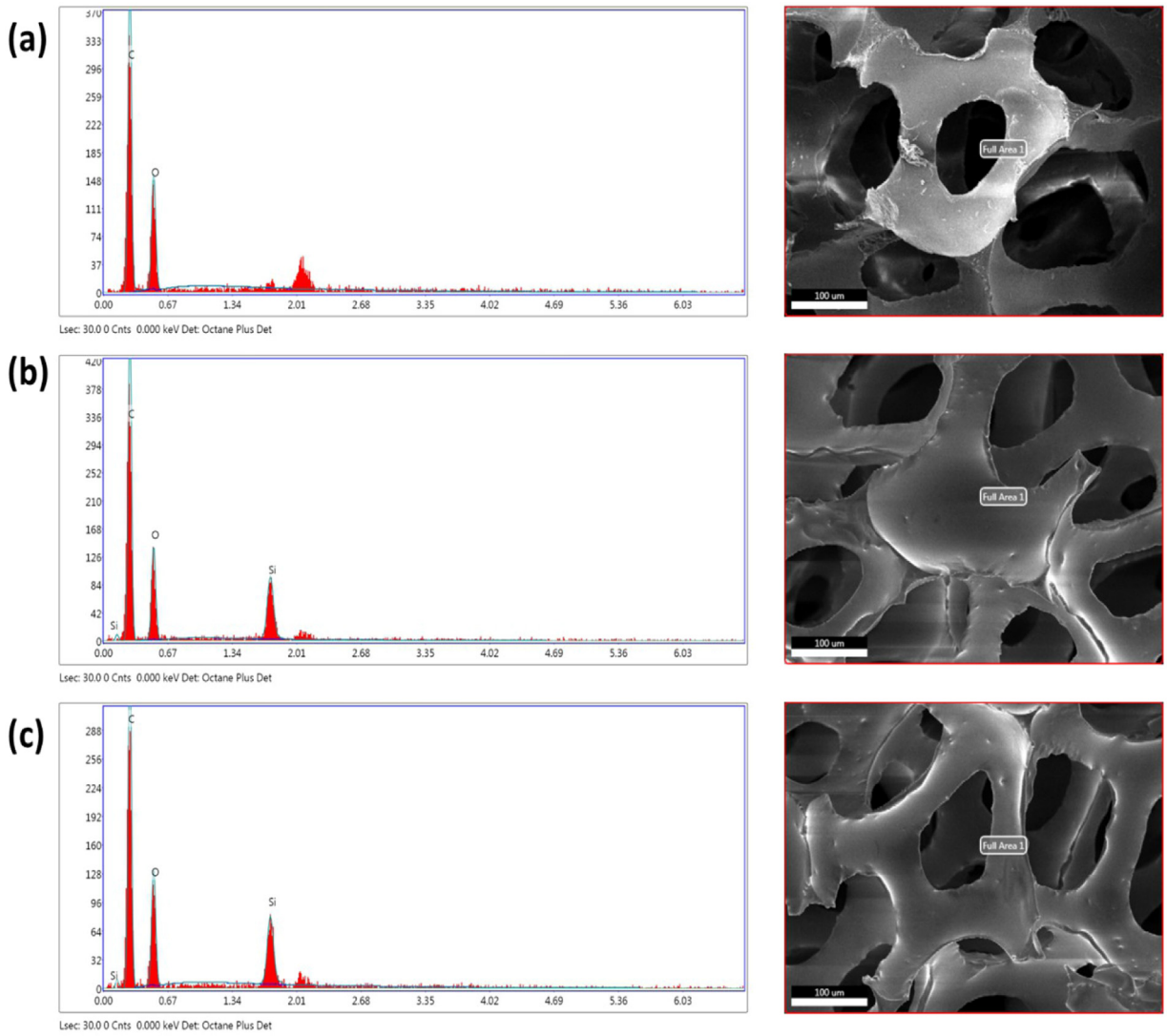

Fig. 10. EDX spectra of (a) C-PU, (b) C-PU/Si-1/HDTMS, and (c) C-PU/Si-2/HDTMS masks.

Table 4
ICP analysis of drained water samples.

Mask type	Silicon concentration (mg/L)	Standard deviation	Intensity (c/s)
C-PU/Si-1/HDTMS	0.030	0.009	32.4
C-PU/Si-2/HDTMS	0.031	0.004	33.6

3.6. Drainage analysis

The modified masks were immersed and soaked in DI water for half an hour. After squeezing the mask samples, the degree of leakage of used chemicals was analyzed in terms of the silicon concentration in the drained water. ICP-MS analysis detected insignificant quantities of silicon in the drained water samples (Table 4). These results indicate that insignificant leaching of Si from the modified masks occurred during the investigation. It is concluded that the stability of the surface modifiers (Si/HDTMS) on the mask surface is significant which suggests that the anti-droplet phenomenon should last for a considerable time. Subsequent FTIR analysis was performed to investigate any other chemical drainage. There is no difference between the FTIR spectra of the unmodified and modified masks, as indicated in Fig. 14. This result confirms the high stability of the coating on the mask surface.

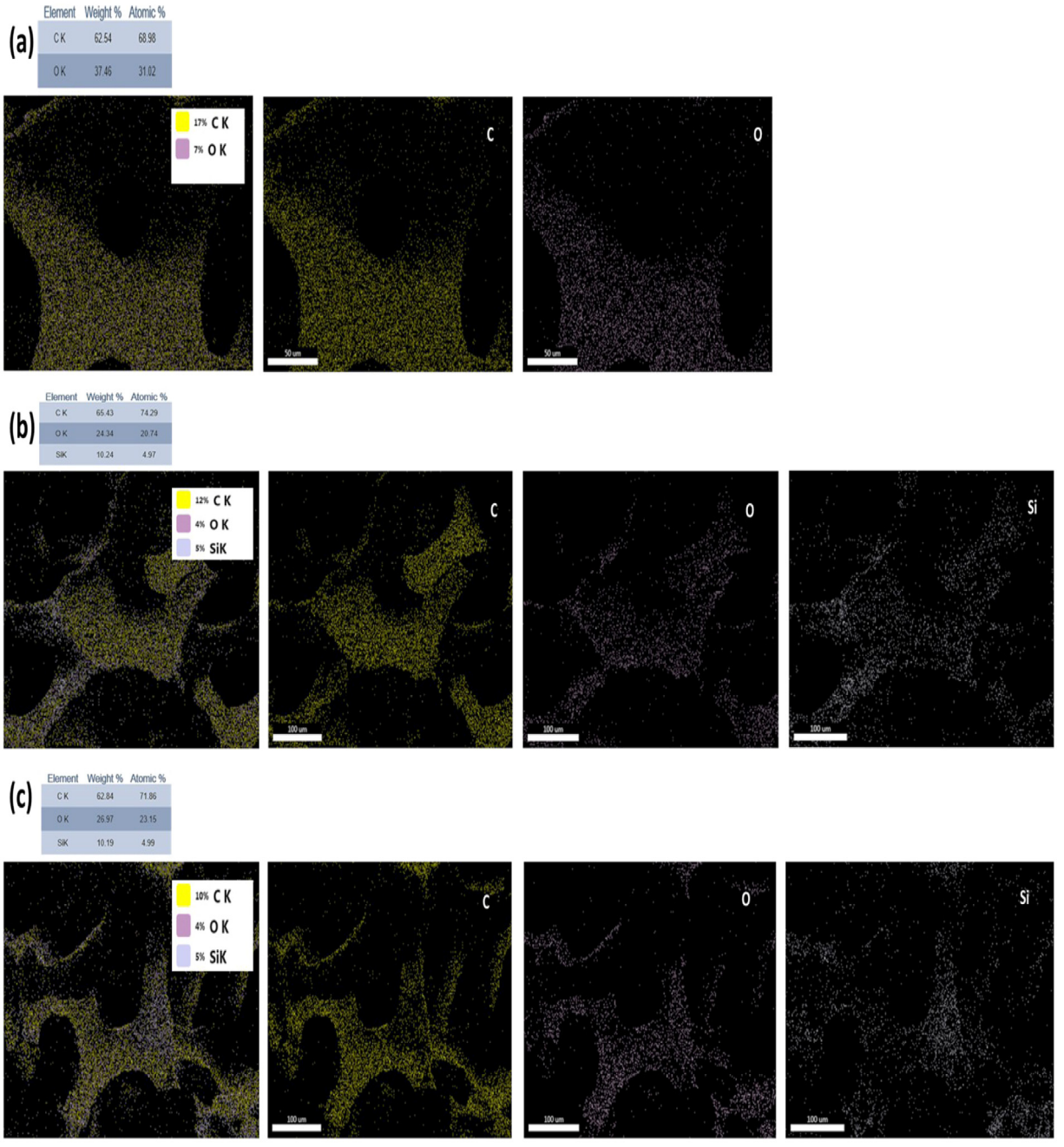

Fig. 11. EDX mapping for verification of desired elements present in unmodified and modified masks.

The stability of the coating was further demonstrated in terms of the average water contact angle after immersing the mask samples in DI water for 30 min. Note the insignificant decrease in the water contact angle for the modified masks (C-PU/Si/HDTMS) (Fig. 15). The average water contact angle value of the modified masks (C-PU/Si-1/HDTMS and C-PU/Si-2/HDTMS), before and after immersion, reduces by only 1.7% and 1.2%, respectively, demonstrating the stable hydrophobic and anti-droplet behavior of modified masks. The unmodified mask (C-PU) shows greater tendency toward surface and pore wetting which reduces its efficacy as a physical barrier.

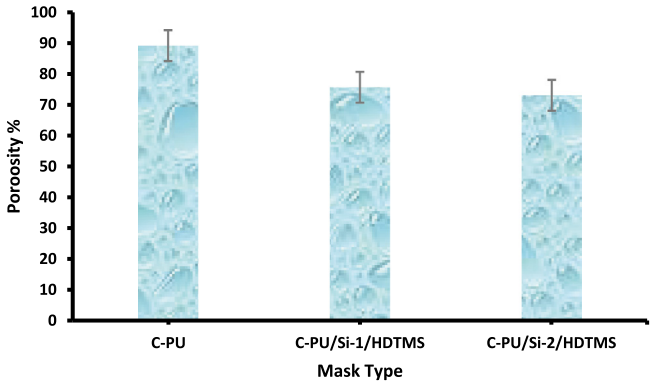

Fig. 12. Evaluation of porosity of various masks.

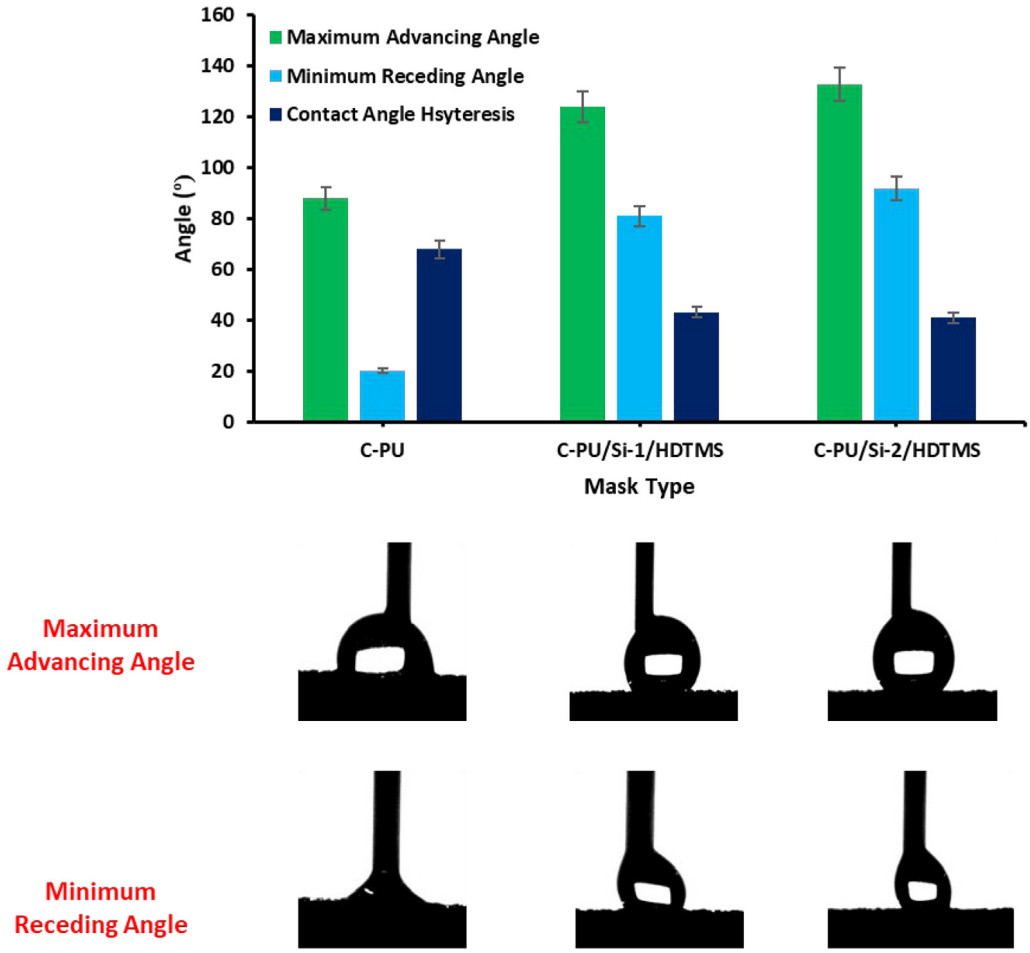

Fig. 13. Analysis of contact angle hysteresis for pristine and modified mask surface.

3.7. Water jet impact test

The durability of the surface coating was qualitatively investigated by conducting a water jet impact test. In this study, the water jet was quickly repelled by the modified mask and the steady local stream did not impair the wetting state and the surface. Interestingly, water droplets adhered to the unmodified mask (C-PU), confirming the adsorbing nature of the mask surface toward water droplets, that result in immediate wetting. The modified mask surface demonstrated greater

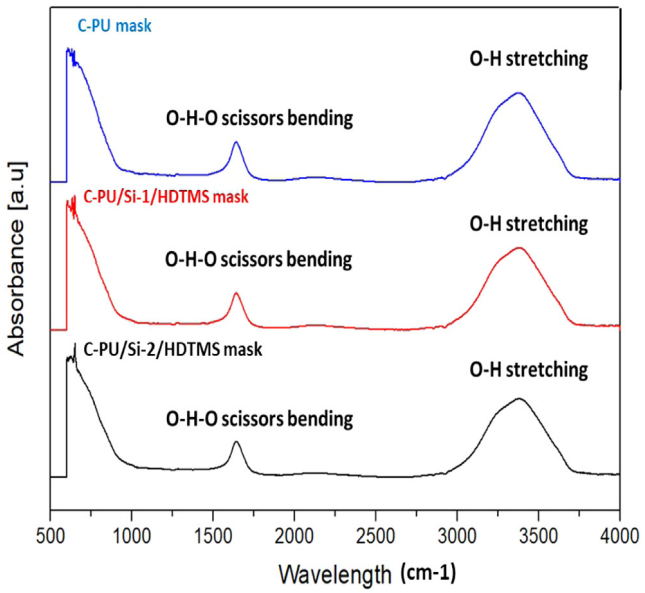

Fig. 14. FTIR spectra of water samples in which the unmodified and modified masks were immersed.

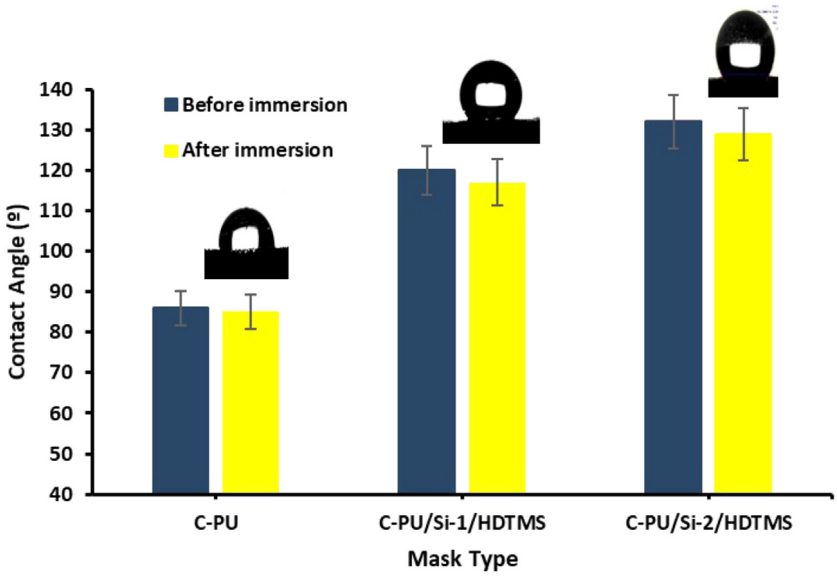

Fig. 15. Investigation of the unmodified and modified masks before and after immersion in DI water.

anti-droplet behavior than the unmodified mask **(Film 1)**. In addition to that, time-lapse video has been updated that justifies the high repellence nature of modified mask where it demonstrated that droplet gets absorbed in pristine mask over a period of 15 min, whereas, there is a negligible change in droplet shape in case of modified mask (C-PU/Si/HDTMS). This illustrates the hydrophobic nature of C-PU/Si/HDTMS mask compared to that of unmodified mask. The video not only indicates the wetting state of modified mask but also suggests high water repellence nature. The trend shown in video was found to be similar as observed in Fig. 6.

4. Conclusion

In this study, an anti-droplet, hydrophobic mask coating was developed for application on a C-PU masks. The coating was derived from a silica sol, formed by hydrolysis of TEOS, and a HDTMS solution. The average pore size of the masks showed negligible change after modification confirming the high breathability of the modified masks (C-PU/Si/HDTMS).

The modified masks achieved maximum water resistance and maintained a high-water contact angle (132°) for a longer period of time than that of the unmodified mask. The engineered surface demonstrated high anti-droplet efficiency against water splatter. Furthermore, the reusability of the modified masks was analyzed in terms of the water contact angle achieved after immersion. The drainage test showed insignificant leaching of the Si coating suggesting strong interaction between the polyurethane and surface modifiers and SEM micrographs confirmed that the modification had minimal effect on the mask morphology, allowing maximum air flow. Finally, the modified mask exhibited self-cleaning ability as a result of the low sliding angle of the inclined surface. These results indicate that surface wetting has been mitigated; accordingly, the proposed coating for C-PU masks has great potential to improve infection control, especially in the medical field.

CRediT authorship contribution statement

Saikat Sinha Ray: Conception and design of study, Acquisition of data, Analysis and/or interpretation of data, Writing - original draft. **You-In Park:** Acquisition of data, Writing - review & editing. **Hosik Park:** Acquisition of data, Writing - review & editing. **Seung-Eun Nam:** Analysis and/or interpretation of data, Writing - review & editing. **In-Chul Kim:** Conception and design of study, Writing - original draft. **Young-Nam Kwon:** Conception and design of study, Analysis and/or interpretation of data, Writing - original draft.

Declaration of competing interest

The authors declare that they have no known competing financial interests or personal relationships that could have appeared to influence the work reported in this paper.

Acknowledgment

This above research was financially aided and backed by the National Research Foundation (NRF) of Korea as funded by the Ministry of Education, Science and Technology (NRF2018R1D1A1B07043609). The authors are thankful for their constant support. Approval of the version of the manuscript to be published (Saikat Sinha Ray, You-In Park, Hosik Park, Seung-Eun Nam, In-Chul Kim, Young-Nam Kwon).

Appendix A. Supplementary data

Supplementary material related to this article can be found online at https://doi.org/10.1016/j.eti.2020.101093.

References

Allison, A.L., Ambrose-Dempster, E., Aparsi, D.T., Bawn, M., Casas Arredondo, M., Chau, C., Chandler, K., Dobrijevic, D., Hailes, H., Lettieri, P., 2020. The environmental dangers of employing single-use face masks as part of a COVID-19 exit strategy.
Ammayappan, L., Chakraborty, S., Pan, N.C., 2020. Silica nanocomposite based hydrophobic functionality on jute textiles. The J. Text. Inst. 1–12.
Anon, 2020, W.Y.F.C. CORRECTLY, How to Safely Wear and Take Off a Cloth Face Covering.
Aydin, O., Emon, M.A.B., Saif, M.T.A., 2020. Performance of fabrics for home-made masks against spread of respiratory infection through droplets: a quantitative mechanistic study. medRxiv.
Bahrambeygi, H., Rabbi, A., Nasouri, K., Shoushtari, A.M., Babaei, M.R., 2013. Morphological and structural developments in nanoparticles polyurethane foam nanocomposite's synthesis and their effects on mechanical properties. Adv. Polym. Technol. 32, E545–E555.
Baji, A., Agarwal, K., Oopath, S.V., 2020. Emerging developments in the use of electrospun fibers and membranes for protective clothing applications. Polymers 12, 492.
Berkalp, O.B., 2006. Air permeability & porosity in spun-laced fabrics. Fibres Text. East. Eur. 14, 81.
Cascella, M., Rajnik, M., Cuomo, A., Dulebohn, S.C., Di Napoli, R., 2020. Features, Evaluation and Treatment Coronavirus (COVID-19), Statpearls [Internet]. StatPearls Publishing.
Choi, C.K., 2010. Comparison between sioc thin film by plasma enhance chemical vapor deposition and SiO2 thin film by fourier transform infrared spectroscopy. J. Korean Phys. Soc. 56, 1150–1155.
Clayton, K.N., Salameh, J.W., Wereley, S.T., Kinzer-Ursem, T.L., 2016. Physical characterization of nanoparticle size and surface modification using particle scattering diffusometry. Biomicrofluidics 10, 054107.
Dias, R.C.M., Góes, A.M., Serakides, R., Ayres, E., Oréfice, R.L., 2010. Porous biodegradable polyurethane nanocomposites: preparation, characterization, and biocompatibility tests. Mater. Res. 13, 211–218.
Eikenberry, S.E., Mancuso, M., Iboi, E., Phan, T., Eikenberry, K., Kuang, Y., Kostelich, E., Gumel, A.B., 2020. To mask or not to mask: Modeling the potential for face mask use by the general public to curtail the COVID-19 pandemic. Infect. Dis. Model..
El-Atab, N., Qaiser, N., Badghaish, H.S., Shaikh, S.F., Hussain, M.M., 2020. A flexible nanoporous template for the design and development of reusable anti-COVID-19 hydrophobic face masks. ACS Nano.
Gaurav, K., Mittal, G., Karn, A., 2020. A short review on the development of novel face masks during COVID-19 pandemic.
Green, D., Lin, J., Lam, Y.-F., Hu, M.-C., Schaefer, D.W., Harris, M., 2003. Size, volume fraction, and nucleation of stober silica nanoparticles. J. Colloid Interface Sci. 266, 346–358.
Guo, J.Z., Song, K., Liu, C., 2018. Polymer-Based Multifunctional Nanocomposites and their Applications. Elsevier.
Huang, Q.-L., C.-f. Xiao, s. Feng, X., Hu, X.-Y., 2013. Design of super-hydrophobic microporous polytetrafluoroethylene membranes. New J. Chem. 37, 373–379.
MacIntyre, C.R., Cauchemez, S., Dwyer, D.E., Seale, H., Cheung, P., Browne, G., Fasher, M., Wood, J., Gao, Z., Booy, R., 2009. Face mask use and control of respiratory virus transmission in households. Emerg. Infect. Dis. 15, 233.
Makkonen, L., 2017. A thermodynamic model of contact angle hysteresis. J. Chem. Phys. 147, 064703.

Marmur, A., Della Volpe, C., Siboni, S., Amirfazli, A., Drelich, J.W., 2017. Contact angles and wettability: towards common and accurate terminology. Surf. Innov. 5, 3–8.
Mishra, R., Militky, J., 2018. Nanotechnology in Textiles: Theory and Application. Woodhead Publishing.
Nazeeri, A.I., Hilburn, I.A., Wu, D.-A., Mohammed, K.A., Badal, D.Y., Chan, M.H., Kirschvink, J.L., 2020. An efficient ethanol-vacuum method for the decontamination and restoration of polypropylene microfiber medical masks & respirators. medRxiv.
Neacşu, I.A., Nicoară, A.I., Vasile, O.R., Vasile, B.Ş., 2016. Inorganic micro-and nanostructured implants for tissue engineering. In: Nanobiomaterials in Hard Tissue Engineering. Elsevier, pp. 271–295.
Nishiura, H., Linton, N.M., Akhmetzhanov, A.R., 2020. Serial interval of novel coronavirus (COVID-19) infections. Int. J. Infect. Dis.
Rothan, H.A., Byrareddy, S.N., 2020. The epidemiology and pathogenesis of coronavirus disease (COVID-19) outbreak. J. Autoimmun. 102433.
Shajari, M., Rostamizadeh, K., Shapouri, R., Taghavi, L., 2020. Eco-friendly curcumin-loaded nanostructured lipid carrier as an efficient antibacterial for hospital wastewater treatment. Environ. Technol. Innov. 100703.
Shakak, M., Rezaee, R., Maleki, A., Jafari, A., Safari, M., Shahmoradi, B., Daraei, H., Lee, S.-M., 2020. Synthesis and characterization of nanocomposite ultrafiltration membrane (PSF/PVP/SiO2) and performance evaluation for the removal of amoxicillin from aqueous solutions. Environ. Technol. Innov. 17, 100529.
Sinha Ray, S., Lee, H.-K., Kwon, Y.-N., 2020. Review on blueprint of designing anti-wetting polymeric membrane surfaces for enhanced membrane distillation performance. Polymers 12, 23.
Sohrabi, C., Alsafi, Z., O'Neill, N., Khan, M., Kerwan, A., Al-Jabir, A., Iosifidis, C., Agha, R., 2020. World Health Organization declares global emergency: A review of the 2019 novel coronavirus (COVID-19). Int. J. Surg..
Tucker, B., Hermann, M., Mainguy, A., Oleschuk, R., 2020. Hydrophobic/hydrophilic patterned surfaces for directed evaporative preconcentration. Analyst 145, 643–650.
Wang, H., Zhou, H., Liu, S., Shao, H., Fu, S., Rutledge, G.C., Lin, T., 2017. Durable, self-healing, superhydrophobic fabrics from fluorine-free, waterborne, polydopamine/alkyl silane coatings. RSC Adv. 7, 33986–33993.
W.H. Organization, Coronavirus disease 2019 (COVID-19): situation report, 72, 2020.
Xie, Z., Yang, Y.X., Zhang, H., 2020. Mask-induced contact dermatitis in handling COVID-19 outbreak. Contact Dermatitis.
Xu, L., Wang, L., Shen, Y., Ding, Y., Cai, Z., 2015. Preparation of hexadecyltrimethoxysilane-modified silica nanocomposite hydrosol and superhydrophobic cotton coating. Fibers Polym. 16, 1082–1091.
Xu, L., Zhuang, W., Xu, B., Cai, Z., 2012. Superhydrophobic cotton fabrics prepared by one-step water-based sol–gel coating. J. Text. Inst. 103, 311–319.